

Field observations to establish the impact of fluvial flooding on potentially toxic element (PTE) mobility in floodplain soils

Article

Accepted Version

Creative Commons: Attribution-Noncommercial-No Derivative Works 4.0

Ponting, J., Verhoef, A. ORCID: <https://orcid.org/0000-0002-9498-6696>, Watts, M. J. and Sizmur, T. ORCID: <https://orcid.org/0000-0001-9835-7195> (2022) Field observations to establish the impact of fluvial flooding on potentially toxic element (PTE) mobility in floodplain soils. Science of the Total Environment, 811. 151378. ISSN 0048-9697 doi: 10.1016/j.scitotenv.2021.151378 Available at <https://centaur.reading.ac.uk/101040/>

It is advisable to refer to the publisher's version if you intend to cite from the work. See [Guidance on citing](#).

To link to this article DOI: <http://dx.doi.org/10.1016/j.scitotenv.2021.151378>

Publisher: Elsevier

All outputs in CentAUR are protected by Intellectual Property Rights law, including copyright law. Copyright and IPR is retained by the creators or other copyright holders. Terms and conditions for use of this material are defined in the [End User Agreement](#).

www.reading.ac.uk/centaur

CentAUR

Central Archive at the University of Reading

Reading's research outputs online

Field observations to establish the impact of fluvial flooding on potentially toxic element (PTE) mobility in floodplain soils

Jessica Ponting^{1,2*}, Anne Verhoef¹, Michael J. Watts² and Tom Sizmur¹

¹ Department of Geography and Environmental Science, University of Reading, Reading, UK

² Inorganic Geochemistry, Centre for Environmental Geochemistry, British Geological Survey, Nottingham, UK

Abstract

Inundation of river water during flooding deposits contaminated sediments onto floodplain topsoil. Historically, floodplains were considered an important sink for potentially toxic elements (PTEs). With increasing flood frequency and duration, due to climate change and land use change, it is important to understand the impact that further flooding may have on this legacy contamination. In this study a field-based approach was taken, extracting soil pore waters by centrifugation of soils sampled on multiple occasions from multiple locations across a floodplain site, which lies adjacent to the River Loddon in southeast England. Flooding generally decreased pore water PTE concentrations and significantly lower pore water concentrations of Cd, Cu, and Cr were found post-flood compared to pre-flood. The dominant process responsible for this observation was precipitation with sulphides resulting in PTE removal from the pore water post-flood. The changes in pH were found to be associated with the decreased pore water concentration of Cu, which suggests the pH rise may have aided adsorption mechanisms or precipitation with phosphates. The impact of flooding on the release and retention of PTEs in floodplain soils is the net effect of several key processes occurring concurrently. It is important to understand the dominant processes that drive mobility of individual PTEs on specific floodplains so that site-specific predictions can determine the impact of future floods on the environmental fate of legacy contaminants.

Keywords; Fluvial flood, Groundwater flood, Legacy contaminants, Mobilisation, Pore water, Hazard

1. Introduction

Floodplain soils are often contaminated with potentially toxic elements (PTEs) such as arsenic (As), cadmium (Cd), cobalt (Co), copper (Cu), chromium (Cr), nickel (Ni), lead (Pb), and zinc (Zn). These are generally released into the environment from anthropogenic sources (Álvarez-Ayuso et al., 2012; Förstner, 2004; Prabakaran et al., 2019; Rennert et al., 2017). Floodplains located in urban catchment areas are contaminated from sources including wastewater/sewage treatment plants, factories using alloys, metal mining, landfills, and road surface runoff from tyre and brake emissions into the river (Hurley et al., 2017; Rowland et al., 2011; Stuart and Lapworth, 2011). Soils have the ability to retain

PTEs and their mobility is affected by pH, their concentration in the soil, cation exchange capacity, organic matter and inorganic interfaces, e.g. clays, metal oxides, metal carbonates and metal phosphates (Bradl, 2004; Stietiya, 2010). The mobilisation of PTEs in floodplain soils, even when at relatively low concentrations, may cause adverse ecological impacts for soil microorganisms, plants, and both terrestrial and aquatic fauna; affecting the function of their endocrine, nervous, and respiratory systems (He et al., 2019; Ortiz Colon, 2016; Tack, 2010; Tóth et al., 2016). A decrease in the mobility of essential PTEs (e.g. Cu, Mn, Zn and Fe) that are also important micronutrients for plants, could result in deficiencies that impair plant function and reduce yields, as well as reduce soil productivity by altering the microbial community (Alloway, 2013; Cornu et al., 2017; Palansooriya et al., 2020).

Climate and land management changes are contributory factors to current and predicted increases in flooding, largely because the effects of a greater intensity and duration of rainfall is exacerbated by urbanisation-driven land use and agricultural practices (O'Connell et al., 2007; Schober et al., 2020; Sparovek et al., 2002). Floodplains are important areas for flood risk management. However, these areas are also a potential environmental risk if flooding results in the remobilisation of legacy contamination from the soils (Ponting et al., 2021; Schober et al., 2020). When floodplain soils undergo inundation, PTE mobility can increase, or decrease, depending on the element (Abgottspon et al., 2015; Beesley et al., 2010; Rinklebe et al., 2016), the floodplain topography (Ciszewski and Grygar, 2016; Du Laing et al., 2009) and the duration of flooding (Ciszewski and Grygar, 2016; Indraratne and Kumaragamage, 2017; Kelly et al., 2020; Shaheen and Rinklebe, 2014). Concentrations of dissolved PTEs may decrease during a flooding event, as a result of a 'dilution effect'; when an increased volume of water is present, and therefore a lower concentration of PTEs is observed. This increase in water volume and subsequent dilution, is not expected to affect the solubility of PTEs. Alternatively, PTE mobility can increase during a flooding event due to flushing of contaminated soil/sediment and subsequent mechanisms for release into solution (Resongles et al., 2015). A review of the literature on this topic concluded that the mobility of PTEs in floodplain soils change during and after inundation due to the net effect of five key processes (Ponting et al., 2021): 1) soil redox potential for which decreases can directly alter the speciation, and hence mobility, of redox sensitive PTEs (e.g. As and Cr), 2) soil pH for which an increase usually reduces the mobility, through increased chelation of metal cations (e.g. Cd^{2+} , Cu^{2+} , Ni^{2+} , Pb^{2+}), 3) dissolved organic matter which can mobilise PTEs that are strongly bound to soil particles, 4) iron and manganese hydroxides undergoing reductive dissolution, thereby releasing adsorbed and co-precipitated PTEs, and 5) reduction of sulphate, which immobilises PTEs due to the precipitation of metal sulphides.

Much of the understanding about the influence of flooding on PTE mobility in floodplains has come from laboratory experiments undertaken in mesocosms. These studies report an increase in PTEs mobility, however, often involve short-exposure time and static temperature and soil water conditions (Frohne et al., 2011; Ponting et al., 2021; Rinklebe and Du Laing, 2011). The extrapolation of laboratory-based findings to field situations can be difficult; although this has been done in studies on mine impacted soils (Cadmus et al., 2016; González-Alcaraz and van Gestel, 2015; Hooda, 2010; Lynch et al., 2014; O'Connell et al., 2007; Simms et al., 2000; Small et al., 2015).

The aim of this study was to investigate the impact of flooding on the mobility of PTEs from floodplain soil downstream from an urban catchment by identifying changes to pore water PTEs concentrations pre-flood, during a flood event and post-flood. The objective was to observe and understand the mechanisms by which PTEs are mobilised or immobilised during a flooding event and post-flood.

2. Methodology

2.1. Site

The Loddon Meadow site used in this study is a floodplain downstream of a lowland urban catchment in England and is part of the Loddon Floodplain Monitoring and Modelling Platform. The Loddon Meadow is located adjacent to the River Loddon, a tributary of the River Thames, to the south of Reading, in southeast England, United Kingdom (Figure 1A and B; 51°24'47.6" N, 0°55'10.6" W). The Loddon Catchment contains sub-urban, agricultural and semi-natural grassland areas. The dominant land covers (34,030 ha) are arable land and improved grassland (The Wildlife Trusts Hampshire & Isle of Wight, 2003). The underlying geology is predominantly clay, silt, sand, and gravel sediments, with chalk in the upper reaches. The soil texture at the Loddon Meadow site have been previously classified as silty loam using laser granulometry method (Kelly et al., 2020). Under the original Soil Survey of England and Wales classification the soils were classified as argillic gley soil (soil series 0841b, Hurst), (Cranfield University, 2021). The Soil Survey of England and Wales classifications have been correlated and reclassified using the World Reference Base, 2006 Tier 1 Version as a Gleysols. Indeed, the soils on the site are classified as being influenced by surface water/groundwater and categorised as Floodzone 3 (high probability of flooding; Figure SI-1). The Loddon Meadow is a floodplain that generally floods annually with the extent and frequency of flooding depending on interrelated environmental conditions (i.e. precipitation, river and groundwater levels, and soil moisture stores).

There are multiple current and historic sources of contamination to the river from within the catchment, including effluents from wastewater sewage treatment plants, chrome alloy plating industries, landfills situated on previous gravel extraction sites, contaminated runoff from urbanised areas, and military establishments (Kelly et al., 2020). The Loddon Meadow floods intermittently

during the winter and occasionally during the summer. Flooding prior to this study was likely to have occurred in April 2018 (Figure SI-2). The extent of flooding is closely linked to the microtopography (soil surface level variation) and elevation of different parts of the floodplain (Figure 1C) (Moser et al., 2007; Schumann et al., 2019; Szabó et al., 2020). The characteristics of the Loddon Meadow soils are provided in Table 1, including pH, organic matter and (pseudo) total concentrations (further detailed in Table SI-1).

Table 1: Soil properties averaged across the Loddon Meadow floodplain site, number of measurements (n) is provided and the +/- standard deviation.

Soil properties	Average on Loddon Meadow floodplain
pH (n=132)	6.53 +/- 0.51
OM (%) (n=120)	16.8 +/- 3.89
Total As (mg/kg) (n=12)	13.5 +/- 3.73
Total Cd (mg/kg) (n=12)	0.56 +/- 0.28
Total Co (mg/kg) (n=12)	13.5 +/- 2.41
Total Cu (mg/kg) (n=12)	25.9 +/- 8.73
Total Cr (mg/kg) (n=12)	35.9 +/- 12.49
Total Ni (mg/kg) (n=12)	21.4 +/- 4.57
Total Pb (mg/kg) (n=12)	67.0 +/- 31.05
Total Zn (mg/kg) (n=12)	137 +/- 40.16

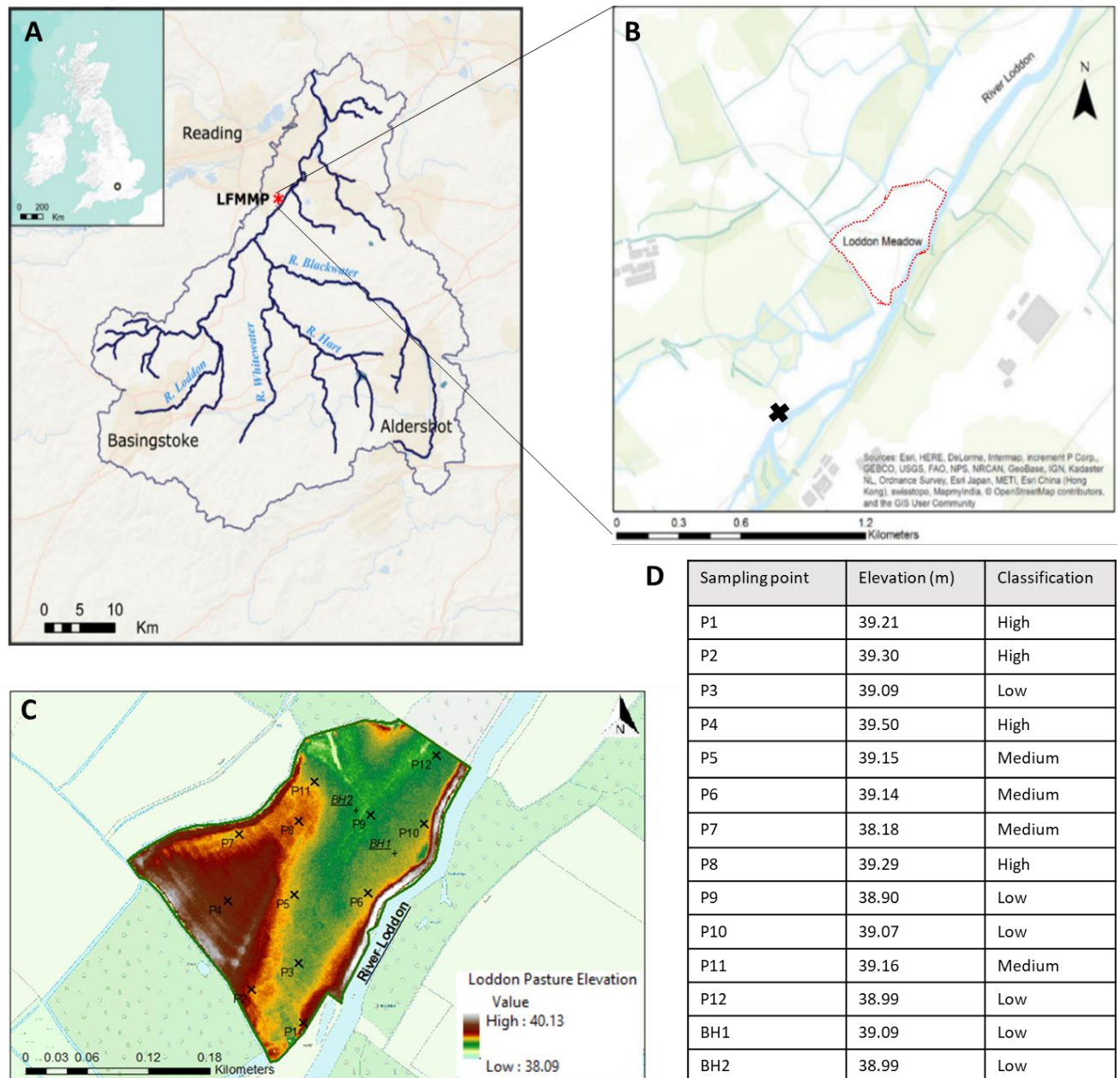


Figure 1; Map of the study site and sampling locations; A) the Loddon Floodplain Monitoring and Modelling platform (LFMMP) showing the regional context (south of Reading in southern England) and the position within the Loddon catchment, B) the local context of the Loddon Meadow site along the northern margin of a section of the River Loddon, with 'X' depicting the location where river water samples were taken upstream from the floodplain, C) a digital elevation model created using Lidar data from Digimap EDINA and hillshade processing in ArcGIS showing the microtopography of the study site. The sampling points P1-14 are shown alongside two boreholes; BH1 and BH2 where groundwater was sampled, and D) a table of sampling points, elevation (metres above ordnance datum) and classification of the locations into 'high', 'medium' and 'low' elevation.

2.2. Sampling

The data used in this paper was collected through the period of December 2018 to March 2019; pre-flood, during the flood, and post-flood. The flood event occurred due to high groundwater levels and overbanking of the River Loddon. There were 5 sampling visits before the flood (pre-flood), one visit during the flood (towards the end of approximately a one-week flood) and 5 sampling visits after the flood (post-flood). Soil properties pre-flood, during the flood and post-flood are presented in Table SI-2. All equipment used for soil sampling, storage of pore water samples, and subsequent analysis of samples was acid washed in 3% HCl overnight prior to use, to prevent contamination from the equipment to the pore water samples.

2.2.1 Soil samples

The 12 sampling locations used throughout the sampling regime (Figure 1C) were selected by creating a Fishnet grid (5m x 5m) in ArcGIS and taking the centre of the grid as the sampling point. The coordinates were put into a Garmin eTrex 10 handheld GPS logger to ensure that the same sampling locations were used during repeat visits. The elevation was determined by creating a digital elevation model using LIDAR data from Digimap and hillshade processing in ArcGIS showing the microtopography of the study site (Figure 1C). These sampling locations represent varying elevations in metres above ordnance datum (Figure 1D).

At each sampling location, 5 soil samples were collected from an approximately 1m² area using a stainless-steel auger to consistently sample the top 30cm of floodplain soil. These 5 samples were combined into 1 composite sample and stored in a cool box before return to the laboratory. Homogenised (~100 g) samples were placed into a Sorvall RC6+ Thermo Scientific (Waltham, Massachusetts, USA) centrifuge at 5,000 rpm (RCF 3830 x g) for 1 hour to extract pore water samples (Di Bonito et al., 2008; Sizmur et al., 2011). Soil pore waters were extracted to determine the free ion concentrations as these are considered the bioavailable metal pools (Hooda, 2010). Analyses conducted on the pore water samples included elements using Inductively Coupled Plasma Mass Spectrometry (ICP-MS), anions using Ion Chromatography (IC), and dissolved organic carbon using the Non-Purgeable Dissolved Organic Carbon (NPOC) method. Details of these analyses are provided below.

2.2.2 Environmental conditions

Daily measurements of river levels are monitored by the Environment Agency at Arborfield Bridge, approximately 1.2 km upstream of the Loddon Meadow floodplain site. These data were accessed remotely (<https://riverlevels.uk/loddon-arborfield-and-newland-arborfield-bridge#.X7udX2j7SUk>). This information, combined with the knowledge that the Loddon Meadow site has an elevation of

between 38 and 40 m above ordnance datum, was used to plan sample collections around the flood event (Figure 2A). When the river level is around 41.19 m or higher, flooding is likely to occur. On the 6th sampling trip (11/02/2019) the floodplain was inundated. This was the only observed flooding event during the sampling period of this study.

River water samples were collected with a Nalgene bottle on a pole from a bridge located upstream of the floodplain (Figure 1B) at two time points (8 am and noon) on each sampling day during the period between November 2018 and March 2019. The water samples collected were transported in a cool box back to the laboratory and then were filtered using a 0.45 µm cellulose nitrate syringe filter and acidified prior to storage in the fridge and further analyses for elements (ICP-MS), anions (IC) and dissolved organic carbon (NPOC), as described below.

There are two boreholes located on the Loddon Meadow Floodplain (Figure 1C). Borehole 1 (BH1) is located closest to the River Loddon and borehole 2 (BH2) is located in the 'low' elevation centre of the floodplain (Figure 1C). Daily measurements of the groundwater levels were monitored remotely using an IMPRESS submersible water pressure transmitter sensor installed in BH1, connected to an Isodaq Technology (Hydro International, Clevedon, UK) Frog RXi-L GPRS-8-channel data logger. The data was accessed via Timeview Telemetry (© 2017 Isodaq Technology, Hydro International), whereas an In-Situ (Fort Collins, Colorado, USA) BaroTROLL sensor was installed in BH2, that required manual downloading and processing. Furthermore, the groundwater levels in the boreholes were regularly 'dipped' manually to allow for correction of the automatically recorded groundwater levels, where required. A BaroTROLL stored in the housing of the 'Frog' datalogger measured atmospheric pressures. These data were also regularly downloaded to correct the BaroTroll data obtained in BH2. This barometric correction was not necessary for the IMPRESS sensor. The groundwater levels were above the ground level on two occasions during this sampling (between the 2nd and 3rd sampling visit and during the 6th sampling visit) and the groundwater levels were within the top 30 cm of the soil profile during the 9th and 10th sampling visits (Figure 2B).

Groundwater samples were collected from BH1 and BH2 on each sampling day during the period between December 2018 and March 2019. An acid-washed 1 m plastic tube with 60 ml syringe was used to create a vacuum to draw water up from the borehole. The first sample drawn up was used to wash the 500 ml Nalgene sample bottle and then discarded. The groundwater samples collected were transported back to the laboratory in a cool box and then were filtered using a 0.45 µm cellulose nitrate syringe filter. Groundwater samples were then analysed for elements (ICP-MS), anions (IC) and dissolved organic carbon (NPOC), as described below.

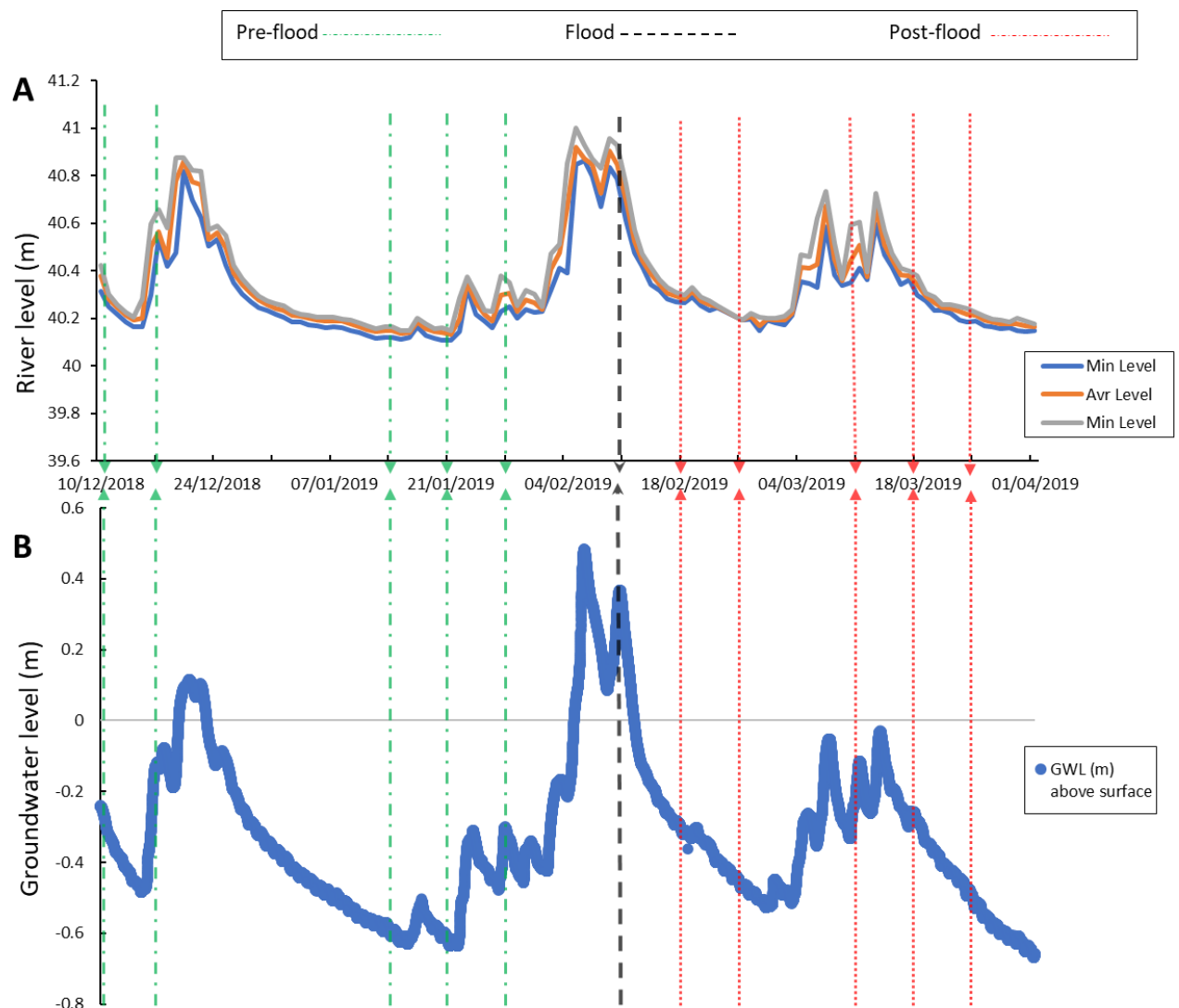


Figure 2; A) Hydrograph showing River Loddon level (m above ordnance datum, where stage datum is 40m) at Arborfield Bridge river level station upstream from the Loddon Meadow floodplain; during the sampling period, B) Groundwater level (m relative to soil surface) averaged from the boreholes on the floodplain. The dot and line green arrows show five sampling dates pre-flood, the dashed line black arrow shows the one sampling date during the flood and the dotted line red arrows show the five sampling dates post-flood.

2.3. Analysis

2.3.1 Laboratory analysis

2.3.1.1 Soil samples

Moisture and organic matter were determined by mass loss after overnight heating to 105 °C and loss on ignition at 500 °C, respectively.

The (pseudo) total concentrations of PTEs in soil samples collected from the floodplain were found through soil digestion by reverse aqua regia method using the CEM Corporation (Matthews, North

Carolina, USA) MARS 6 microwave digestion system followed by ICP (OES and MS) analysis (Sizmur et al., 2019). A limitation of this method is that it can often lead to an underestimation of the total concentrations because aqua regia is unable to dissolve silicates and aluminium and iron oxides to which some elements may be bound (Santoro et al., 2017). Each batch of 30 samples was run alongside a replicate of an in-house reference material (SS 51) that is traceable to a Channel sediment certified reference material (BCR 320 R). We obtained the following recovery rates for As (64%), Cd (81%), Co (106%), Cu (97%), Cr (86%), Ni (86%), Pb (86%), and Zn (92%).

2.3.1.2 Soil porewater, river water, and groundwater

The soil pH, and redox potential were determined immediately following sampling using a Hanna (Woonsocket, Rhode Island, USA) 9125 pH/ORP meter. For the pH reading, two buffer solutions (pH 4 & 7) were used to calibrate the probe and to check for drift, after every 10 samples. For the redox potential, the probe was checked using a redox check solution before measurements on the samples were taken. Measurements were only taken when the redox check solution reading was +476 mV.

Electrical conductivity (EC) is a measure of the proportion of anions and cations in the solution (De Vivo et al., 2008). In addition to EC being part of the experimental data, it was also used to help identify the correct dilutions required for Ion Chromatography (IC) analysis. The samples were allowed to equilibrate to approximately room temperature prior to taking this measurement. For the conductivity, a check solution was made using KCL 0.746 g in 1L. This solution has a known conductivity (1411 μ S) and so was used to check the probe prior to measurement on the samples.

All samples were frozen after pH, redox and EC analysis, and then shipped in batches to the British Geological Survey (BGS), Keyworth via courier for further laboratory analysis. The dissolved organic carbon (DOC) content was measured with a Shimadzu (Kyoto, Japan) TOC-L series TOC analyzer using the NPOC method. The groundwater and river water samples were analysed without dilution as there was a greater sample volume than that collected for the pore waters. All samples were acidified to remove inorganic carbon prior to measurement of DOC with a non-dispersive infrared gas analyser. The limit of detection for the Shimadzu TOC-L and NPOC instrument was 0.5 mg/L. A blank check was run before any samples to avoid contamination within the machine. Standards were made from potassium hydrogen phthalate (total carbon) and sodium hydrogen carbonate and sodium carbonate (inorganic carbon) and DOC calculated as the difference between these measurements.

The concentrations of nitrate (NO_3^-) and sulphate (SO_4^{2-}) were measured in 200 μ l sub-samples by Ion Chromatography (IC) on a Dionex (Sunnyvale, California, USA) AS-AP. Low sample volumes meant dilution was necessary, the dilution was based on the conductivity reading (i.e. twofold dilution for

samples with a conductivity 200-500 μS and fivefold dilution for samples with a conductivity 500-800 μS).

The concentrations of PTEs and other elements (As, Cd, Co, Cu, Cr, Ni, Pb, Zn, Mn, Fe, Al, P, S, Ca, and Mg) were analysed via an Agilent (Santa Clara, California, USA) 8900 Inductively coupled plasma mass spectrometer (ICP-MS). All of the samples were acidified with 1% HNO_3 and 0.5% HCl prior to analysis. The detection limits for the PTEs (As, Cd, Co, Cu, Cr, Ni, Pb, and Zn) are shown in Table SI-3.

2.3.2 Statistical analyses

Data analysis was performed using Microsoft Excel 2019 (descriptive statistics) and SAS software version 9.4 (Linear Mixed effects Mode; LMM). The LMM takes into account the repeated sampling temporally (specific pattern) and spatially (the spatial scatter chosen at random). All of the response (dependent) variable values were log-transformed due to the fact that pore water PTE concentrations followed log-normal distributions. The model also included explanatory factors as model effects; elevation, distance to river, treatment (pre-flood, during the flood or post-flood), soil moisture (proxy for flooding/groundwater level), organic matter, soil pH, redox, conductivity, DOC, as well as pore water concentrations of Fe, Mn, Al, Ca, K, NO_3^- , P and S. The p-values indicate the significance value, any p-values higher than 0.05 are not stated in the results section text, as the trends were not evident.

The percentage change in concentration of each PTE and explanatory factors during (equation 5.1) or post-flood (equation 5.2), compared to pre-flood, was calculated as follows:

$$\% \Delta C_{df} = \frac{C_{df} - C_{bf}}{C_{bf}} \times 100 \quad (5.1)$$

$$\% \Delta C_{af} = \frac{C_{af} - C_{bf}}{C_{bf}} \times 100 \quad (5.2)$$

Where:

C_{df} = concentration during the flood

C_{bf} = concentration before the flood (pre-flood)

C_{af} = concentration after the flood (post-flood)

Principal Component Analysis (PCA) using PRIMER-e (Massey University, Auckland, New Zealand) version 7 was undertaken with the data classified by the position on the floodplain (sampling position P1-14) as well as by elevation ('high' (39.50 m - 39.21 m), 'medium' (39.18 m – 39.14 m), and 'low' (39.09 m – 38.90 m) which was classified prior to analysis (Figure 1D) and by time ('pre-flood', 'flood' and 'post-flood'). The data was normalised in PRIMER-e prior to the PCA and the output visualises the

dataset and allows subsequent interpretation of correlations found between variables in the dataset. A one-way ANOVA (ANOSIM) was used to test spatial and temporal differences in the dataset by comparing the treatment levels (pre-flood, flood, and post-flood), elevation (high, medium, and low) and the treatment and elevation combined. ANOSIM generates an R value between -1 and 1, where zero represents the null hypothesis, a negative value indicates greater variability within the treatment than between different treatments, and a positive value indicates the amount by which the treatments differ.

3. Results

3.1. Porewater concentrations

The Loddon Meadow floodplain is not heavily polluted (Table 1, Table SI-1) with concentrations ranging within natural levels (Rawlins et al., 2012). Therefore, this study investigates whether a flooding event on a typical floodplain downstream of an urban catchment could alter the concentrations of PTEs in soil pore waters. The (pseudo) total concentrations of the PTEs are geospatially mapped across the Loddon Meadow (Figures SI-3 to SI-10).

During the flood, mean pore water concentrations of As, Cu, Cr, Ni and Zn were lower than pre-flood concentrations, whereas the mean concentrations of Cd, Co and Pb increased during the flood, compared to pre-flood concentrations, calculated using equation 5.1 (Figure 3A). However, none of the PTE concentrations in pore waters were statistically significantly different during the flood, compared to pre-flood ($p > 0.05$). When looking at the explanatory variables (Figure 3B), a higher mean pore water concentration of Mn and lower mean pore water concentrations of Fe, Al, S, NO_3^- , Ca, Mg and pH were found during the flood, compared to pre-flood. However, none of these were statistically significant. The pore water concentrations of DOC and P were significantly lower during the flood compared to pre-flood ($p < 0.01$).

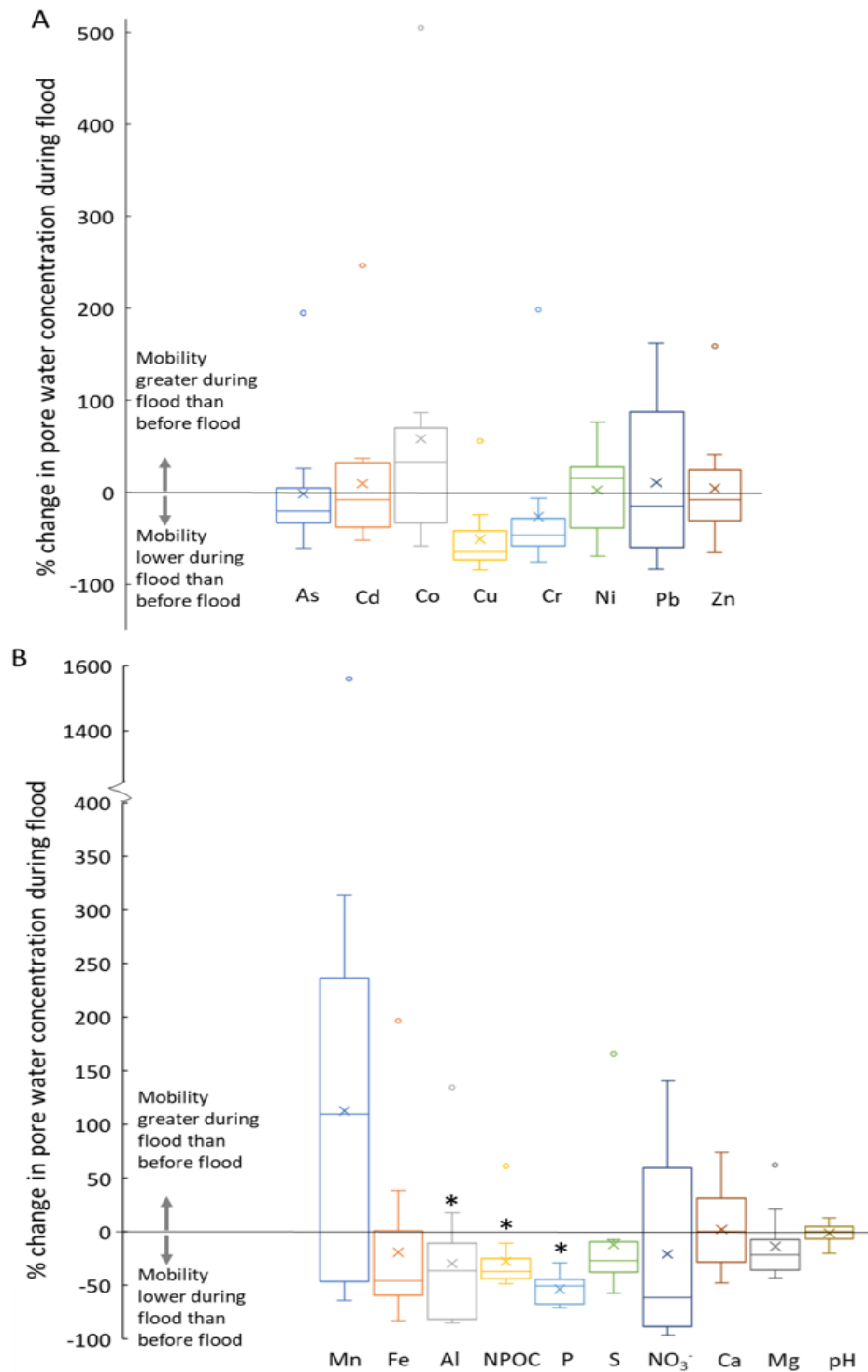


Figure 3; % change in pore water concentration during flood for A) PTEs and B) key explanatory variables. The % change increase or decrease is in relation to the averaged concentration (N=12) found pre-flood. Box and whisker plots show the distribution of data into quartiles (box) and variability outside of the upper and lower quartiles (whiskers). The 'outlier' results (outside of the normal range of values i.e. 1.5 times the inter-quartile range below the 1st quartile or 1.5 times above the 3rd quartile) are represented as dots. The 'x' denotes the mean value and the line across the box is the median value. The * denotes significant differences in concentration ($p < 0.05$).

Post-flood mean pore water concentrations of As, Cd ($p<0.01$), Cu ($p<0.05$), Cr ($p<0.01$), Pb and Zn were lower than pre-flood concentrations, whereas the post-flood mean concentrations of Co and Ni were greater than pre-flood concentrations, calculated using equation 5.2 (Figure 4A). However, none of the PTE concentrations in pore waters were statistically significantly different during the flood, compared to pre-flood ($p>0.05$). When looking at the explanatory variables (Figure 4B), the mean Mn pore water concentrations were found to have remained higher (not significantly) when the floodwater had receded post-flood, compared to concentrations pre-flood. The soil pH slightly increased, meaning that the H^+ ion concentrations decreased, post-flood, compared to pre-flood. The mean pore water concentrations of Fe and Al, were lower post-flood compared to concentrations pre-flood (not significantly) as were the concentrations of DOC ($p<0.05$), P ($p<0.1$), S ($p<0.05$), NO_3^- ($p<0.01$), Ca ($p<0.05$), Mg ($p<0.05$). .

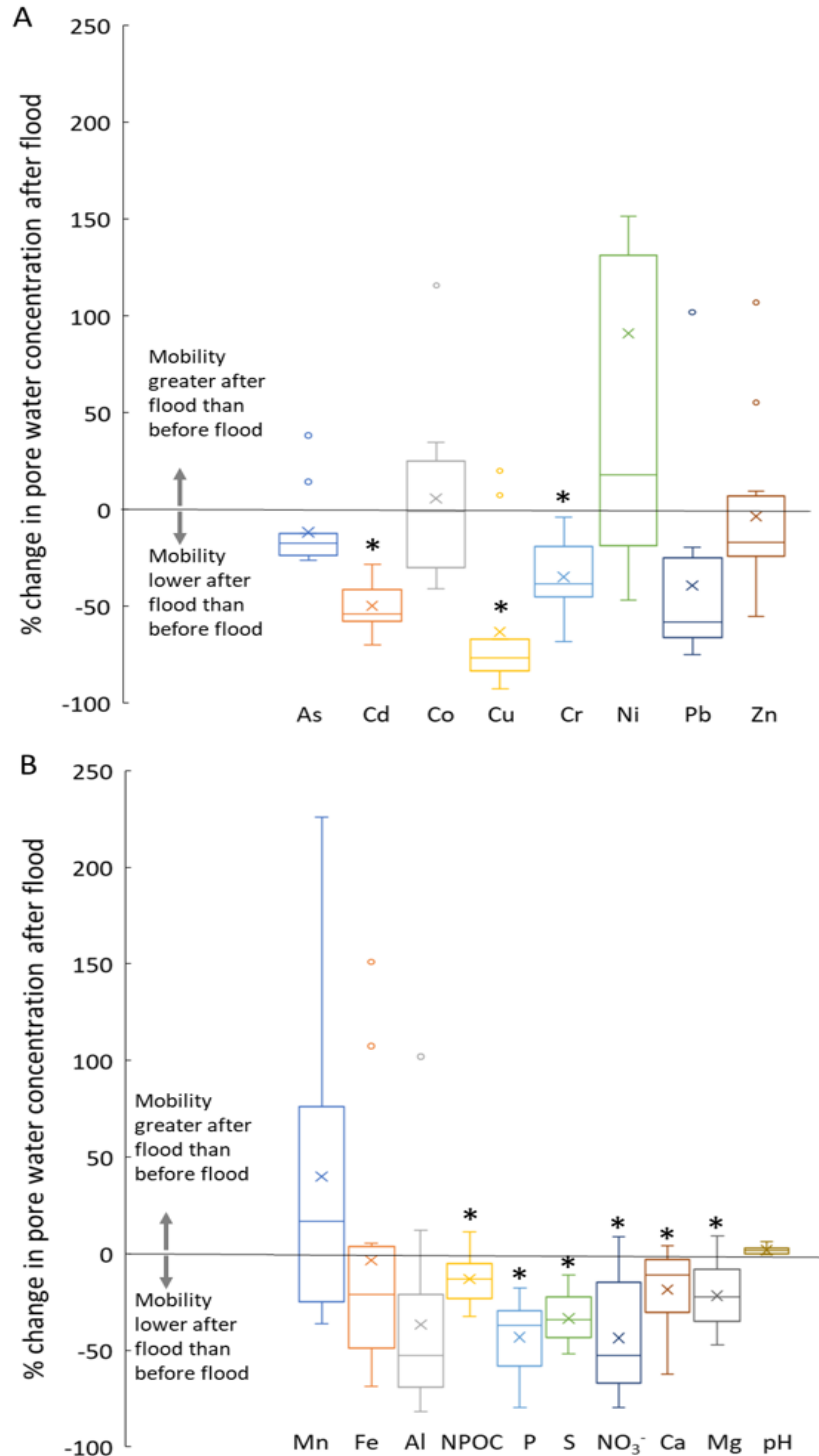


Figure 4; % change in pore water concentration after flooding (post-flood) for A) PTEs B) key explanatory variables. The % change increase or decrease is in relation to the averaged concentration (N=12) found pre-flood. Box and whisker plots show the distribution of data into quartiles (box) and variability outside of the upper and lower quartiles (whiskers). The 'outlier' results (outside of the normal range of values i.e. 1.5 times the inter-quartile range below the 1st quartile of 1.5 times above the 3rd quartile) are represented as dots. The 'x' denotes the mean value and the line across the box is the median value. The * denotes significant differences in concentration ($p < 0.05$).

Temporal (pre-flood, during the flood, post-flood) and spatial (high, medium, low elevation) factors influenced the pore water chemistry on the floodplain (Table SI-4 Analysis of Similarities (ANOSIM)). When the temporal and spatial treatments were combined and the influence on pore water chemistry considered, the flooding event (during the flood) appeared to remove the differences in pore water chemistry seen across the three elevations. These factors were considered in greater detail in the Principal Component Analysis (PCA; Figure 5). Pore water samples collected pre-flood tended to have a positive loading on PC1 (x axis of Figure 5), while samples collected during or post-flood have a negative loading. Pore water samples collected from low elevation locations tended to have a negative loading on PC2 (y axis of Figure 5), while pore water samples collected from medium and high elevation locations tended to have a positive loading. Therefore, it is concluded from the biplot (Figure 5) that time (pre-flood, flood and post-flood) is represented on PC1 and location/elevation (high, medium and low) is represented on PC2. These two principal components (PC1 and PC2), combined, explain 35% of the variability in the dataset. The PCA also identified organic matter, pH, redox and conductivity as important factors explaining the variability in the pore water chemistry.

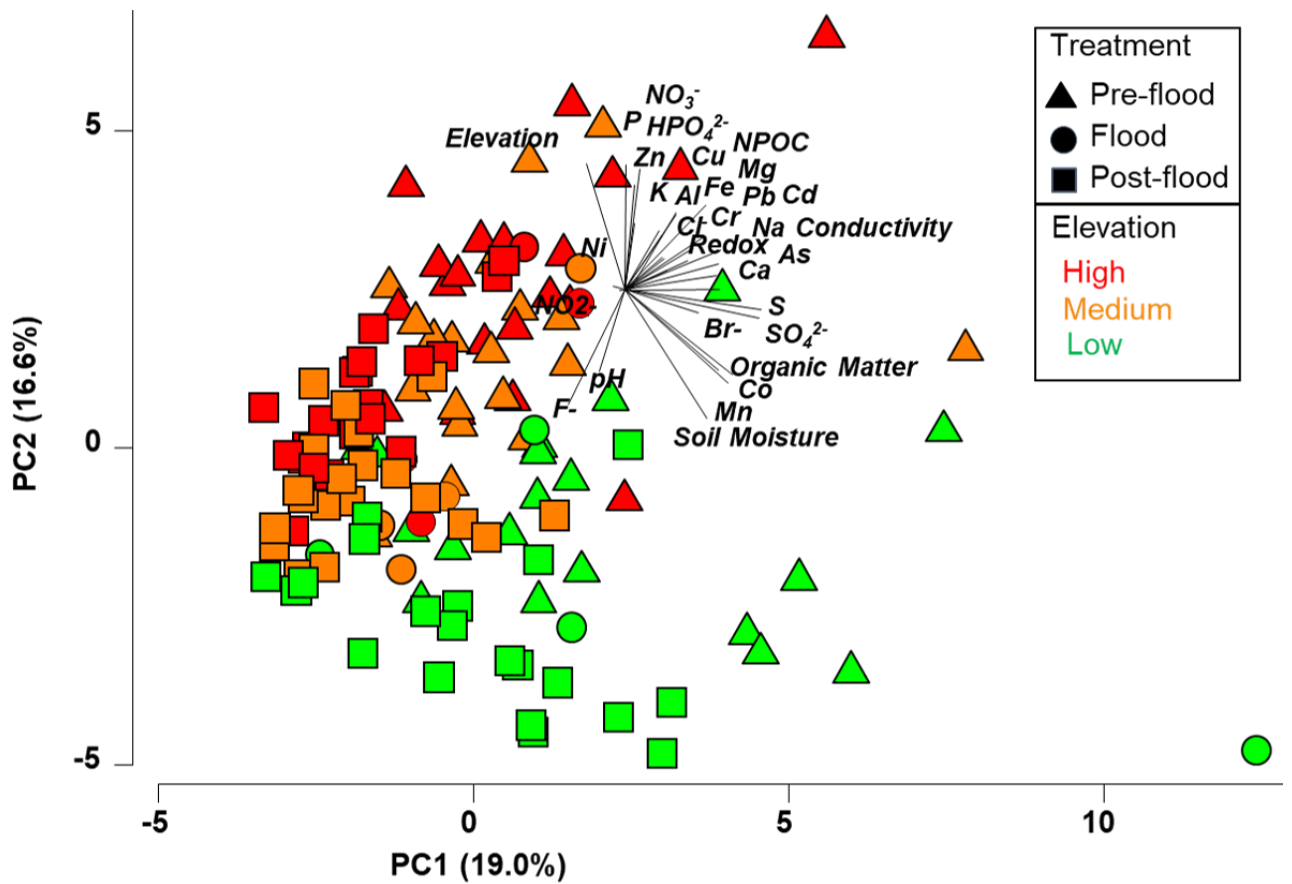


Figure 5; Principal Component Analysis (PCA) biplot, reflecting correlation between PTEs and other explanatory variables at three time points (pre-flood, during flooding and post-flood) and at three elevations on the floodplain (high, medium and low).

The results of Linear Mixed effects Modelling (LMM) are shown in Table 2. The explanatory variables contributing the influence of flooding on each individual PTE are discussed below element by element using a combination of the % changes in pore water concentrations and PCA and LMM statistical outputs to help determine the key process(es) involved in the mobility of each PTE.

340 **Table 2;** Results of mixed model (LMM) analysis. The numbers reported here are the fixed effects ‘estimate’ which means that for every 1 unit increase in an
341 explanatory variable there is either a positive or negative change in PTE concentration in µg/L. The effect size significance (p value) is indicated by * denoting
342 <0.05, ** denoting <0.01 and *** denoting <0.001.
343

Response variable (PTE)	During flood concentration compared to pre-flood	Post-flood concentration compared to pre-flood	Explanatory variables (fixed effects ‘estimate’) & effect size														
			Elevation	Soil moisture	OM	pH	Redox	Conductivity	DOC	Fe	Mn	Al	Ca	K	P	S	NO ₃ ⁻
Arsenic	Decrease	Decrease	0.05	0.002	0.02	-0.001	-0.001	0.00003	0.01***	0.00002	0.001***	0.0004***	-0.006***	0.00002	0.37*	0.004	0.002*
Cadmium	Increase	Decrease	0.47	0.0001	0.03	-0.125	0.0003	0.00035	-0.008	1.909	0.002***	0.00003	-0.00009	0.009	1.29***	-0.0005	0.003
Cobalt	Increase	Increase	-0.04	0.009*	-0.009	0.049	0.0015	0.0006	0.011***	0.00006	0.004***	0.0006***	-0.00571*	-0.008	-0.22	-0.004	-0.004**
Copper	Decrease	Decrease	-0.08	0.0003	0.035	-0.296*	-0.0056	0.0012	0.012	0.00029*	-0.002*	0.00026	0.00224	0.0528***	-0.346	-0.0133	-0.006*
Chromium	Decrease	Decrease	0.046	-0.0103***	0.048***	-0.091	-0.0061***	-0.0011*	0.009*	0.00008	0.002***	0.0007***	0.00097	-0.0083	0.115	-0.0023	0.003*
Nickel	Decrease	Increase	-1.4153*	-0.0132	0.021	-0.017	-0.0003	0.0003	0.008	-0.00006	0.00004	0.0005	0.0043	-0.0201*	0.0421	0.0011	0.409
Lead	Increase	Decrease	-0.2305	0.0107	0.0051***	-0.299***	0.0024	0.00005	-0.0008	0.00019	0.00142*	0.00103***	-0.0124***	0.0029	1.1025***	0.0119	0.003
Zinc	Decrease	Decrease	0.8387	-0.0019	0.0037	-0.079	0.0001	0.00136	-0.0074	0.00017	-0.00052	-0.00024	0.0128	0.0149	0.1624	-0.008	-0.003

3.1.1. Arsenic

The mean pore water concentrations of As were found to decrease (albeit not statistically significantly) both during the flood and post-flood (Table SI-5). A significant positive correlation was found between As and DOC, this could be due to pH having a similar effect on both As and DOC solubility (both decreased during and post-flood). Alternatively As concentrations could have been affected by the reduction of As(V) to As(III) during anoxic conditions.

A positive correlation was found between As and P pore water concentrations. However, rather than this being an explanatory variable it is likely that these elements are affected by the same processes (DOC complexation and reductive dissolution of Fe oxides), since phosphate is chemically very similar to arsenate (Strawn, 2018).

3.1.2. Cadmium

The mean Cd pore water concentrations were found to increase during the flooding and subsequently decreased (significantly) post-flood (Table SI-5). There is a strong positive correlation between Cd and Mn, and this is a significant variable in the LMM (Figure 5, Table 2). They both have a positive loading on PC1 (pre-flood, during the flood, post-flood; Figure 5), reflecting greater pore water concentrations pre-flood.

A significant positive correlation was found between Cd and P concentrations in pore water. They both have a positive loading on PC2, reflecting greater pore water concentrations at high elevation (Figure 5) and they both decreased post-flood (Table SI-5 and SI-6). This relationship may suggest that Cd is being immobilised by the phosphate. However, phosphate fertilisers also contain trace amounts of Cd, so rather than this being an explanatory variable, the positive correlation we found may just infer the existence of a source of Cd in this floodplain soil from agricultural land in the catchment.

3.1.3. Cobalt

The Co pore water concentrations were found to increase (albeit not significantly) during the flood and post-flood (Table SI-4). The mobility appears to be strongly linked to that of Mn (Table SI-6), as Co has a high affinity for Mn oxides. Cobalt and Mn concentrations in pore waters significantly positively correlate with each other (LMM; Table 2). They both have a positive loading on PC1 (pre-flood, during the flood, post-flood) and negative loading on PC2 (elevation; Figure 5). Therefore, when Mn oxides were reductively dissolved the concentrations of both Mn and Co increased in pore water (Figure 3 and 4), particularly in the low elevation sampling points pre-flood (Figure SI-5), likely influenced by the high groundwater levels (Figure 2B).

3.1.4. Copper

The Cu pore water concentrations were found to decrease both during the flood and (significantly) post-flood (Table SI-5). The LMM identified pH as a significant explanatory variable influencing Cu mobility, with a negative correlation found (Table 2). The pH did increase slightly post-flood (albeit not significantly) and this may have increased the Cu sorption, resulting in low concentrations in the pore water.

There was a significant positive correlation between Cu and Fe (LMM; Table 2) and these are both positively loaded on PC1 and PC2 (Figure 5) meaning greater pore water concentrations pre-flood and at high elevation. The Cu may have been adsorbed to Fe oxides and a release of Cu pre-flood (Figure SI-6) may be explained by an increase in Fe in solution resulting in reductive dissolution when the ground water levels were high (within the top 30 cm of soil; Figure 2B).

3.1.5. Chromium

The Cr pore water concentrations were found to decrease both during the flood and (significantly) post-flood (Table SI-5). During flooding the soil moisture increased and this was found to have a significant negative correlation with Cr (LMM; Table 2), possibly linked to reducing conditions.

There was a positive correlation between Cr and DOC and this was a significant positive variable in the LMM (Table 2). They both have a positive loading on PC1 (pre-flood, during the flood, post-flood; Figure 5) meaning greater concentrations were found pre-flood. The concentration of Cr and DOC were both decreased during the flood and post-flood, meaning that Cr may have been reduced in the presence of fresh DOC during flooding and removed from the pore water solution due to the reduction in DOC.

Despite the overall Cr pore water concentrations being found to decrease, a significant positive correlation between Cr and Mn concentrations (LMM; Table 2) may explain why there were high Cr concentrations in the pore waters collected pre-flood (Figure SI-7), as they both had a positive loading on PC1 (Figure 5). Therefore, reductive dissolution of Mn oxides may have released Cr into the pore waters.

3.1.6. Nickel

The Ni pore water concentrations decreased during the flood and then increased post-flood (Table SI-5). However, the LMM does not provide strong evidence for why we observed changes in Ni mobility. Spatial and temporal variations did not appear to explain the changes in Ni concentrations found (Figure SI-8). It is possible that Ni was released during reductive dissolution of oxides, however there

were insufficient sulphides formed to precipitate it to a significant degree. The precipitation of Cu and Zn with sulphides would be preferential to the Ni sulphide formation. Therefore, the Ni mobility remained high post-flood, before Fe and Mn oxides reform. In soil solution, Ni generally occurs as the free ion (Ni^{2+}) which is stable and forms strong associations to redox sensitive species and dissolved organic ligands (e.g. carboxylic acids, amino acids and fulvic acids) (Rinklebe and Shaheen, 2017).

3.1.7. Lead

The Pb pore water concentrations were found to slightly increase during flooding and subsequently decreased (albeit not significantly) post-flood (Table SI-5). There was a positive correlation between Pb pore water concentrations and soil organic matter. The Pb mobility was likely controlled by desorption and dissolution processes during the flood, with adsorption and removal from the solution post-flood due to the slight increase in pH. There was a significant positive correlation between Pb and Mn concentrations (LMM; Table 2) and these have a positive loading on PC1 (pre-flood, during the flood, post-flood; Figure 5), so reductive dissolution could explain the increased pore water concentrations pre-flood (Figure SI-9).

There was also a significant positive correlation between Pb and P. They both had a positive loading on PC2 (elevation; Figure 5) so there may have been immobilisation of Pb from pore waters due to precipitation of Pb phosphates, a stable mineral substance, removing it from pore water solution post-flood (Andrunik et al., 2020).

3.1.8. Zinc

The Zn pore water concentrations decreased (albeit not significantly) during the flood and post-flood (Table SI-5). However, the LMM does not provide evidence for why we observed this, with no significant correlations with explanatory variables. The Zn and Cu pore water concentrations appear to correlate and therefore the mechanisms controlling the mobility of Cu may also explain the mobility of Zn (Shaheen et al., 2014). For example, the influence of pH on sorption and complexation with DOC. Zn pore water concentrations were found to increase on one sampling occasion pre-flood and one sampling occasion post-flood, across the whole floodplain (Figure SI-10) which suggests there are mechanisms to release Zn into the pore water that have not been established through the explanatory variables measured in the study.

3.2. Concentrations in the river and ground water

The PTE concentrations in the river water (Table SI-7) and groundwater (Table SI-8) were generally orders of magnitude lower than the pore water PTE concentrations from the floodplain soil. Most of the PTE concentrations did not significantly change over time in the river water (Figure 6A) or

groundwater (Figure 6B). However, in the river water samples higher mean concentrations were found during the flood and decreased concentrations post-flood for Cd ($p=0.003$), Co ($p=0.001$), Cr ($p=0.041$) and Pb ($p<0.01$), which may provide some evidence against the dilution effect (increased volumes of river water resulting in a lower concentration of PTEs through dilution) in the river during the flood event (Figure 2A). In the groundwater samples higher mean concentrations of Co ($p=0.052$) were found during the flood and post-flood compared to pre-flood. There were also high groundwater levels post-flood (within the top 30 cm of the soil; Figure 2B). This would have caused (near-) saturated conditions in the surface soil, partly due to the capillary fringe being of a significant size in this soil, due to the soils relatively high clay content and related pore-size distribution. Therefore, the groundwater levels may have influenced the soil pore water concentrations through reduction processes, despite there being no observable flooding above the ground. The high groundwater levels may have caused a release of Co from the floodplain soil into the pore waters with subsequent leaching downwards into the groundwater.

From this analysis, it was concluded that PTEs in the river and groundwater were not at high enough concentrations to have significantly increased the concentrations we observed in floodplain soil pore waters. An increase in the concentrations of PTEs observed in the pore water samples during the flooding event or post-flood were more likely due to release from the floodplain soil than brought in during the inundation of river water or via rising groundwater levels. The low concentrations combined with the increased water volume during the flooding might result in dilution of the soil pore water PTE concentrations, explaining the decreased concentrations found during flooding.

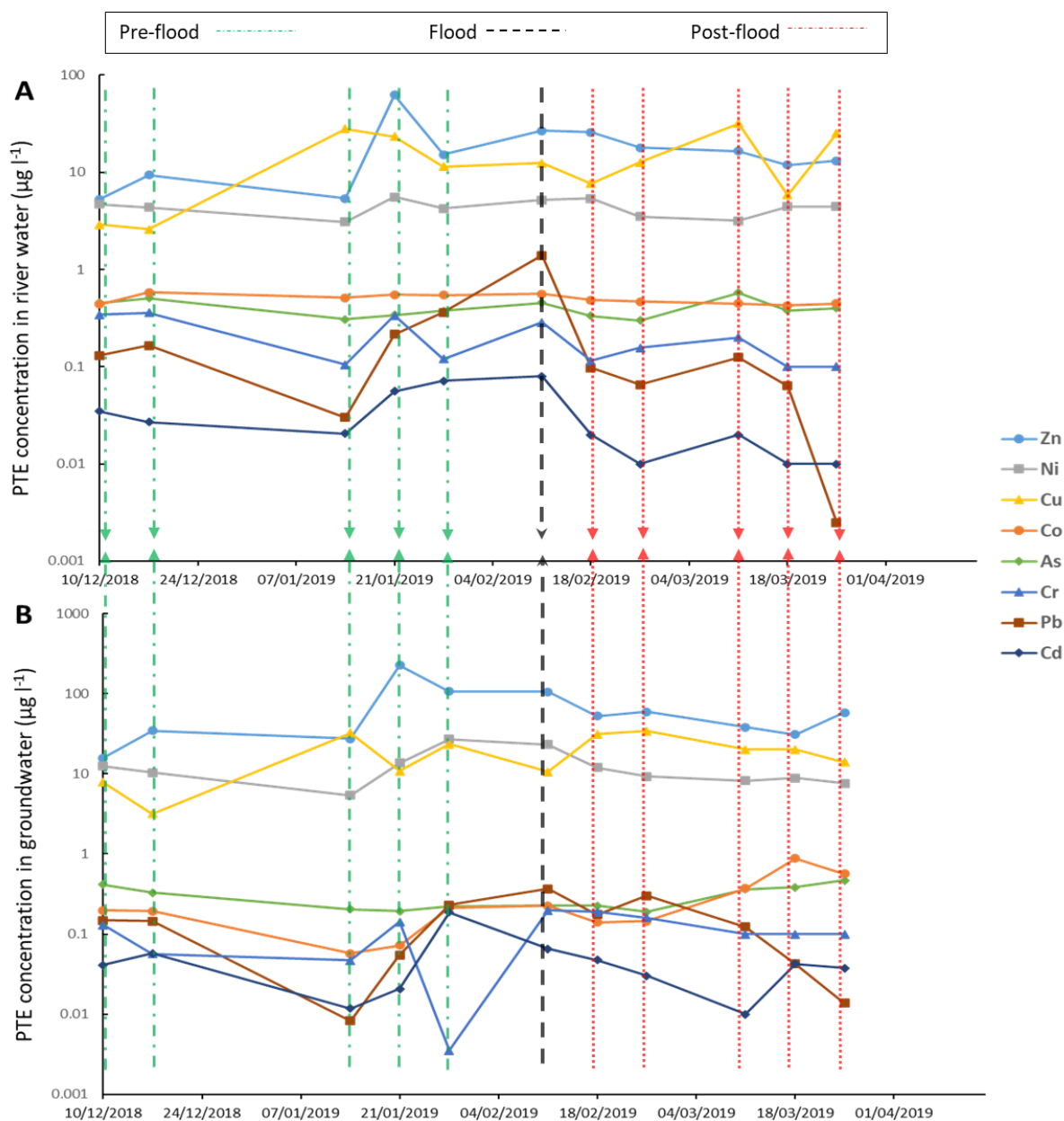


Figure 6; A) PTE concentrations in the river water ($\mu\text{g l}^{-1}$) and B) PTE concentrations in the ground water ($\mu\text{g l}^{-1}$). The dot and line green arrows show five sampling dates pre-flood, the dashed line black arrow shows the one sampling date during the flood and the dotted line red arrows show the five sampling dates post-flood.

4. Discussion

This study has provided field-based evidence of the effect of flooding on the mobility of PTEs from floodplain soils, and the results suggest that there were no significant increases in PTEs mobility during the flooding, and therefore no evidence to support the idea that floodplains become a source for PTEs due to flooding events. This is an interesting result because evidence from laboratory mesocosm studies have suggested there is potential for mobilisation of PTEs as a result of flooding (Frohne et al., 2011; Izquierdo et al., 2017; Rinklebe et al., 2010; Weber et al., 2009). The overall concentrations of PTEs decreased during the flooding and this may be due to dilution effect from river water inundation and high groundwater levels (Balaban et al., 2019). The temporal comparisons (pre-flood, during the flood, and post-flood) provides evidence to suggest that the influence of a flooding event on PTE mobility continues after the floodwaters recede.

Overall, there were higher concentrations of PTEs found in the pore waters collected at low elevation than at the medium or high elevations, so it was inferred that the microtopography (a proxy for flood duration) is an important factor influencing the mobility of PTEs. The entire floodplain sampled for this study was inundated during the flooding event and we found that this meant the differences in PTE pore water concentrations due to elevation (microtopography) were not observed at this time point, likely due to mixing in the floodwater. The changes in concentrations of individual PTEs over time and across the floodplain may be explained due to a net effect of five key processes: redox potential, soil pH, complexation with dissolved organic matter, Fe/Mn reductive dissolution and sulphate reduction (Ponting et al., 2021). The contribution of each of these will be discussed in turn in the sections below.

4.1. Soil redox potential

The soil redox potential is directly affected by flooding because water fills the pore space, reducing the concentration of dissolved oxygen, which is exhausted by organisms. Pore water Cr concentrations decreased during the flood and post-flood, and were found to be linked to redox potential. This observation was expected as Cr is a redox sensitive element (Frohne et al., 2015; Lee et al., 2005; Trebien et al., 2011). Reducing conditions can also immobilise and sequester Cr through reductive precipitation mechanisms (Matern and Mansfeldt, 2016). However, speciation analysis to see whether Cr (III) or Cr (VI) was present in the pore water samples was not conducted, Cr (III) is the more stable form and tends to occur in soils with high OM. A separate study on the same floodplain site found that pore water samples contained only Cr (III) (Kelly et al., 2020). Furthermore, DOC may act as electron donor to reduce Cr (VI) to Cr (III) (Maranguit et al., 2017; Zhang et al., 2017) and DOC was generally

high at all sampling points, across the floodplain. Arsenic, Fe and Mn are also redox sensitive elements, these concentrations may have also been influenced by the reducing conditions and DOC.

4.2. Soil pH

During flooding the pH is known to increase due to H^+ ions being consumed (Mohamed and Paleologos, 2018). This study found the pH increased slightly after the floodwater recedes post-flood. The pH increase might be due to the amount of exchangeable Ca, Mg and K (Wood et al., 2004). The size of the increases in pH may be dependent on flood duration (Kashem and Singh, 2001) and therefore the slight increase that we observed may suggest that the flooding had not been long enough to significantly alter pH. If the pH had increased to very alkaline conditions, this could have increased the mobility for most of the PTEs (Król et al., 2020). During flooding events, H^+ ions are available for consumption in processes such as the reduction of Fe and Mn. The concentrations of H^+ were lower post-flood (increase pH) which suggests that these processes took place in this study. The changes in pH were found to be significantly associated with the decreased pore water concentrations of Cu and Pb, which suggests the pH rise may have aided adsorption mechanisms, resulting in strong binding to soil mineral and organic matter surfaces, or precipitation with P (Andrunik et al., 2020; Cirelli et al., 2009; Koupai et al., 2020; Zia-ur-Rehman et al., 2015). Significant associations of As, Cd and Pb were found with P. Therefore these PTEs may have precipitated as metal phosphates resulting in decreased bioavailability (Andrunik et al., 2020; Van Groeningen et al., 2020; Zia-ur-Rehman et al., 2015). In weakly acidic to neutral pH soils, as sampled on the Loddon Meadow (average 6.53; Table 1; Table SI-2), clay minerals and Fe(III)/Mn(II) oxides are also important mineral sorbent phases for PTEs e.g. Cd; its divalent form is soluble but can form complexes with organics and oxides (Mulligan et al., 2001; Van Groeningen et al., 2020). The concentrations of Cd in the soil were low (Table 1, Table SI-1) and therefore adsorption processes were likely controlling (im)mobility (Van Groeningen et al., 2020).

4.3. Dissolved Organic Matter

Organic matter is an important site of PTE retention in soils. However, due to complexation by soluble organic matter, the addition of dissolved organic matter in soil solution can also act as a chelating agent and therefore be associated with mobilisation of PTEs (Beck et al., 2008; Grybos et al., 2009; Newsome et al., 2020; Sherene, 2010). The higher the concentration of DOC in the soil solution, the greater the pore water concentration of PTEs that bind with DOC in solution. The composition of DOC is complex due to microbial decomposition/degradation processes of organic substances (e.g. root exudates) in soil (Antoniadis and Alloway, 2002). As concentrations, which decreased both during the flood and post-flood, were found to be strongly correlated with DOC. This observation supports the notion that arsenate ($As(V)$) was the dominant form in the floodplain pore waters because it has a

greater affinity for sorption to soil minerals (Indraratne and Kumaragamage, 2017; Williams et al., 2011). A significant association between As pore water concentrations and redox potential was not found, so this flooding event might not have been long enough for reduction from As(V) to As(III) to occur and subsequently increase the mobility of As in the floodplain soils. Cr concentrations decreased both during the flood and post-flood, which was correlated with soil organic matter and DOC. As DOC will change over time, but soil organic matter does not (in the timescale of this sampling), the correlation with DOC is likely to relate to temporal changes whereas the correlation with soil organic matter is likely to relate to spatial differences. This finding suggests that as there was less DOC in solution the equilibrium between the solid and liquid phase for Cr shifts towards the solid phase (i.e. the pore water has less capacity to contain Cr because there is less DOC in solution) (Di Bonito et al., 2008; Icopini and Long, 2002; Wuana et al., 2011).

4.4. Reductive dissolution (Fe/Mn)

An increase in concentrations of Fe and Mn were found in the soil pore water during flooding, comparable to the increases reported in studies across a range of soil types (Amarawansa et al., 2015; Du Laing et al., 2007; Indraratne and Kumaragamage, 2017; Stafford et al., 2018). It was found that the increase in concentration was much higher for Mn than for Fe, as was also found by Indraratne and Kumaragamage (2017). Reductive dissolution appears to be a predominant process for the mobilisation of PTEs in this study, releasing adsorbed As, Cd, Co, and Pb into the pore waters, particularly at the low elevation sampling points (Figure SI-3, SI-4, SI-5 and SI-9 respectively), even if the net effect of multiple mechanisms during the flood or post-flood was to reduce the pore water concentrations of these elements. The process of reductive dissolution is bacterially-induced and has been reported to have an effect on As mobilisation, releasing the mobile form of As during a flood but also immobilising it due to co-precipitation post-flood when oxic conditions return (Chowdhury et al., 2018; Frohne et al., 2011). The Cd and Pb concentrations during the flooding were also likely controlled by desorption and dissolution processes, influenced by the reducing conditions of the flood and association with Mn oxides (Frohne et al., 2011; Furman et al., 2007; Stafford et al., 2018).

In flooded soils Mn(II) is often the major cation in the soil solution and has therefore been expected to compete with PTE cations (e.g. Cd(II) and Zn(II)) for adsorption to mineral surfaces (Van Groeningen et al., 2020). Post-flood, during aeration of the soil, Fe(II) is oxidised by O₂ much more rapidly than Mn(II); this means that Mn can persist for prolonged periods and continue to act as a competing cation with PTEs, or form new Mn-containing solid phases that leads to a net increase in the sorption of PTEs e.g. Cd (Van Groeningen et al., 2020). Dissolution of Co has been closely linked to that of Mn (Beck et al., 2010; Newsome et al., 2020); when Mn oxides are reductively dissolved, Co is released into the

solution (Cornu et al., 2009; Shaheen et al., 2016). There has been an evaluation of the effect that competition with Co for ion exchange sites has on Cr. It is thought that increasing Co concentrations, coupled with a decreasing availability of surface area for precipitation as the dissolution of Mn occurs, results in lower Cr(III) adsorption to Mn oxides. This subsequently results in lower Cr(VI) formation which would have increased the Cr mobility (Shaheen et al., 2016; Trebien et al., 2011). Studies on PTEs are commonly focused on a single metal, but they occur simultaneously in the environment and so an understanding of interactions is an important consideration (Aprile et al., 2019).

4.5. Precipitation of metal sulphides

Flooded soils can result in immobilisation of PTEs through precipitation with insoluble sulphides (Bunquin et al., 2017; Du Laing et al., 2009; Indraratne and Kumaragamage, 2017; Lair et al., 2009). The concentration of S in the pore water (all total S was found to be sulphate when compared using regression analysis ($R^2=98.08\%$, $p<0.01$)) decreased during the flood and (significantly) post-flood, suggesting that there was sulphate reduction to sulphide occurring during this study. The S concentrations negatively correlated with Cd, Cu and Cr (albeit not significantly; Table 2). These PTEs significantly decreased post-flood and therefore it is possible that they have precipitated with sulphides during the flood and removed from the pore water post-flood. When aerobic conditions return, sulphides can be oxidised by microbes resulting in soluble PTEs (e.g. Cd and Zn) being released (Emerson et al., 2017; Lynch et al., 2014). This may explain some increased concentrations of these elements in the pore waters in the lower elevation a number of weeks after the floodwater recedes post-flood (Figure SI-4 and SI-10), but not enough to prevent the overall finding that PTE concentrations decreased post-flood, compared to during the flood.

4.6. River water and Groundwater concentrations

The concentrations of PTEs in the river water were measured and found to be orders of magnitude lower than in the pore water samples. Although these samples are a snapshot of the concentrations in the river at the time of sampling, they suggest that the concentrations of PTEs that were found in the pore waters were most likely concentrations originating from the floodplain soil, rather than being deposited onto the floodplain during the flood event. The top 30 cm of soil was sampled for this study and the groundwater levels (Figure 2B) were within the top 30 cm during pre-flood (2nd sampling visit before flooding) and post-flood (3rd sampling visit after flooding) at the location of boreholes. Therefore, reduction mechanisms may have taken place in the soil prior to flooding or continued after the water aboveground recedes particularly at lower elevation areas of the field.

There were greater concentrations of Pb, Ni and Cr measured in the groundwater during the flood and greater concentrations of Co post-flood, compared to pre-flood. Therefore, the Loddon Meadow floodplain may have released contaminants into the groundwater, which is an environmentally sensitive media (Kotuby-Amacher and Gambrell, 1989), especially because river water and groundwaters are highly connected in floodplain areas. The PTE concentrations will depend strongly on the flow between the river and groundwater. At times the river is feeding the groundwater and other times it is the other way around.

5. Conclusions

Floodplain soils have long been considered a sink for contamination discharged into rivers through sedimentation during flooding events (Frohne et al., 2011; Izquierdo et al., 2017; Rinklebe et al., 2010; Weber et al., 2009)(Balaban et al., 2019). This study demonstrates that the influence of a flooding event on PTE mobility continues after the floodwaters recede post-flood. A significant reduction in mobility of Cd, Cu and Cr was found post-flood and this was due to an increase in pH, a reduction in DOC, and the precipitation of metal sulphides. There were differences in the concentrations of PTEs in soil pore waters observed across the floodplain, suggesting that a number of different processes influencing mobility are acting at the same time across a spatial area. This study highlights the need for more field-based studies to monitor soil pore waters from floodplains pre-flood, during the flood, and post-flood because the impact of flooding on mobility of PTEs may not be as clear-cut and consistent as laboratory studies have previously indicated. The impact of flooding on PTE mobility is likely to be the result of a net effect of multiple processes occurring simultaneously, so while we have observed some increases to PTEs mobility, the overall net effect was found to be a decrease in concentrations because immobilising processes were dominant (i.e. precipitation and adsorption). Further field monitoring of different soil types on floodplains is required to support modelling exercises that would improve predictive capabilities.

Acknowledgements

Jessica Ponting is supported by a NERC SCENARIO PhD studentship, with CASE support from the British Geological Survey Universities Funding Initiative. The authors acknowledge the technical laboratory support from Dr Tom Kelly and Elliott Hamilton at BGS and Anne Dudley and Karen Gutteridge at Reading University. Statistical advice was provided by Sandro Leidi at Statistical Services Centre Ltd.

Supplementary Material

The following can be found in supplementary material:

Figure SI-1: Environment Agency Flood Map for the Loddon Meadow
 Figure SI-2: Levels from 1st January 2018 to 1st April 2019 to show river and ground water levels
 Table SI-1: Soil pseudo-total (aqua regia) concentrations for the sampling points across the Loddon Meadow floodplain site.
 Table SI-2: Soil properties; moisture organic matter and pH across the Loddon Meadow floodplain pre-flood (averaged 5 sampling visits), during the flood and post-flood (averaged 5 sampling visits).
 Table SI-3: Detection limits for PTEs using ICP-MS
 Table SI-4: Analysis of similarities (ANOSIM) a one-way ANOVA testing 1) the treatment levels (pre-flood, flood and post-flood) and 2) elevation and 3) treatment with elevation from Principal Component Analysis (PCA).
 Table SI-5: Summary statistics for the concentrations of PTEs ($\mu\text{g l}^{-1}$) found in the floodplain soil pore water during the sampling regime
 Table SI-6: Summary statistics for the concentrations of explanatory variables ($\mu\text{g l}^{-1}$) found in the floodplain soil pore water during the sampling regime
 Table SI-7: Summary statistics for the concentrations of PTEs ($\mu\text{g l}^{-1}$) found in the river water
 Table SI-8: Summary statistics for the concentrations of PTEs ($\mu\text{g l}^{-1}$) found in the ground water
 Figure SI-3: Arsenic concentrations map series, total soil concentrations, pre-flood, during the flood and post flood
 Figure SI-4: Cadmium concentrations map series, total soil concentrations, pre-flood, during the flood and post flood
 Figure SI-5: Cobalt concentrations map series, total soil concentrations, pre-flood, during the flood and post flood
 Figure SI-6: Copper concentrations map series, total soil concentrations, pre-flood, during the flood and post flood
 Figure SI-7: Chromium concentrations map series, total soil concentrations, pre-flood, during the flood and post flood
 Figure SI-8: Nickel concentrations map series, total soil concentrations, pre-flood, during the flood and post flood
 Figure SI-9: Lead concentrations map series, total soil concentrations, pre-flood, during the flood and post flood
 Figure SI-10: Zinc concentrations map series, total soil concentrations, pre-flood, during the flood and post flood

References

- Abgottspon, F., Bigalke, M., Wilcke, W., 2015. Fast colloidal and dissolved release of trace elements in a carbonatic soil after experimental flooding. *Geoderma* 259–260, 156–163.
<https://doi.org/10.1016/J.GEODERMA.2015.06.005>
- Alloway, Brian J., 2013. Sources of Heavy Metals and Metalloids in Soils, in: Alloway, Brain J., Trevors, J.T. (Eds.), . Springer International Publishing, pp. 11–50. https://doi.org/10.1007/978-94-007-4470-7_2
- Álvarez-Ayuso, E., Otones, V., Murciego, A., García-Sánchez, A., Regina, I.S., 2012. Antimony, arsenic and lead distribution in soils and plants of an agricultural area impacted by former mining

activities. *Sci. Total Environ.* 439, 35–43. <https://doi.org/10.1016/J.SCITOTENV.2012.09.023>

Amarawansa, E.A.G.S., Kumaragamage, D., Flaten, D., Zvomuya, F., Tenuta, M., 2015. Phosphorus Mobilization from Manure-Amended and Unamended Alkaline Soils to Overlying Water during Simulated Flooding. *J. Environ. Qual.* 44, 1252–1262. <https://doi.org/10.2134/jeq2014.10.0457>

Andrunik, M., Wołowicz, M., Wojnarski, D., Zelek-Pogudz, S., Bajda, T., 2020. Transformation of Pb, Cd, and Zn minerals using phosphates. *Minerals* 10, 342. <https://doi.org/10.3390/min10040342>

Antoniadis, V., Alloway, B., 2002. The role of dissolved organic carbon in the mobility of Cd, Ni and Zn in sewage sludge-amended soils. *Environ. Pollut.* 117, 515–521. [https://doi.org/10.1016/S0269-7491\(01\)00172-5](https://doi.org/10.1016/S0269-7491(01)00172-5)

Aprile, A., Sabella, E., Francia, E., Milc, J., Ronga, D., Pecchioni, N., Ferrari, E., Luvisi, A., Vergine, M., De Bellis, L., 2019. Combined effect of cadmium and lead on durum wheat. *Int. J. Mol. Sci.* 20. <https://doi.org/10.3390/ijms20235891>

Balaban, N., Laronne, J.B., Feinstein, S., Vaisblat, G., 2019. Dynamics of metals bound to suspended sediments in floods and on channel banks of the ephemeral Wadi Sekher, northern Negev desert, Israel. *CATENA* 172, 243–254. <https://doi.org/10.1016/J.CATENA.2018.08.018>

Beck, A.J., Cochran, J.K., Sañudo-Wilhelmy, S.A., 2010. The distribution and speciation of dissolved trace metals in a shallow subterranean estuary. *Mar. Chem.* 121, 145–156. <https://doi.org/10.1016/J.MARCHEM.2010.04.003>

Beck, M., Dellwig, O., Schnetger, B., Brumsack, H.-J., 2008. Cycling of trace metals (Mn, Fe, Mo, U, V, Cr) in deep pore waters of intertidal flat sediments. *Geochim. Cosmochim. Acta* 72, 2822–2840. <https://doi.org/10.1016/J.GCA.2008.04.013>

Beesley, L., Moreno-Jiménez, E., Clemente, R., Lepp, N., Dickinson, N., 2010. Mobility of arsenic, cadmium and zinc in a multi-element contaminated soil profile assessed by in-situ soil pore water sampling, column leaching and sequential extraction. *Environ. Pollut.* 158, 155–160. <https://doi.org/10.1016/j.envpol.2009.07.021>

Bradl, H.B., 2004. Adsorption of heavy metal ions on soils and soils constituents. *J. Colloid Interface Sci.* 277, 1–18. <https://doi.org/10.1016/j.jcis.2004.04.005>

Bunquin, M.A.B., TANDY, S., BEEBOUT, S.J., SCHULIN, R., 2017. Influence of Soil Properties on Zinc Solubility Dynamics Under Different Redox Conditions in Non-Calcareous Soils. *Pedosphere* 27, 96–105. [https://doi.org/10.1016/S1002-0160\(17\)60299-6](https://doi.org/10.1016/S1002-0160(17)60299-6)

696 Cadmus, P., Clements, W.H., Williamson, J.L., Ranville, J.F., Meyer, J.S., Gutiérrez Ginés, M.J., 2016.
697 The Use of Field and Mesocosm Experiments to Quantify Effects of Physical and Chemical
698 Stressors in Mining-Contaminated Streams. *Environ. Sci. Technol.* 50, 7825–7833.
699 <https://doi.org/10.1021/acs.est.6b01911>

700 Chowdhury, M.T.A., Deacon, C.M., Steel, E., Imamul Huq, S.M., Paton, G.I., Price, A.H., Williams, P.N.,
701 Meharg, A.A., Norton, G.J., 2018. Physiographical variability in arsenic dynamics in Bangladeshi
702 soils. *Sci. Total Environ.* 612, 1365–1372. <https://doi.org/10.1016/j.scitotenv.2017.09.030>

703 Cirelli, F., Holzapfel, E., De Callejo, I., Billib, M., Miretzky, P., Cirelli, A.F., 2009. Phosphates for Pb
704 immobilization in soils: A review View project. <https://doi.org/10.1007/s10311-007-0133-y>

705 Ciszewski, D., Grygar, T.M., 2016. A Review of Flood-Related Storage and Remobilization of Heavy
706 Metal Pollutants in River Systems. *Water. Air. Soil Pollut.* 227, 1–19.
707 <https://doi.org/10.1007/s11270-016-2934-8>

708 Cornu, J.Y., Huguenot, D., Jézéquel, K., Lollier, M., Lebeau, T., 2017. Bioremediation of copper-
709 contaminated soils by bacteria. *World J. Microbiol. Biotechnol.*
710 <https://doi.org/10.1007/s11274-016-2191-4>

711 Cornu, Sophie, Cattle, J., Samouëlian, Anatja, Laveuf, C., Albéric, Patrick, Cornu, S, Samouëlian, A,
712 Guilherme, L., Albéric, P, 2009. Impact of Redox Cycles on Manganese, Iron, Cobalt, and Lead in
713 Nodules. *Soil Sci. Soc. Am. J.* 73. <https://doi.org/10.2136/sssaj2008.0024i>

714 De Vivo, B., Belkin, H.E., Lima, A., 2008. Environmental Geochemistry: Site Characterization, Data
715 Analysis And Case Histories, Environmental Geochemistry: Site Characterization, Data Analysis
716 and Case Histories. Elsevier. <https://doi.org/10.1016/B978-0-444-53159-9.X0001-0>

717 Di Bonito, M., Breward, N., Crout, N., Smith, B., Young, S., 2008. Overview of Selected Soil Pore
718 Water Extraction Methods for the Determination of Potentially Toxic Elements in
719 Contaminated Soils. Operational and Technical Aspects., in: Environmental Geochemistry: Site
720 Characterization, Data Analysis and Case Histories. Elsevier Inc., pp. 213–249.
721 <https://doi.org/10.1016/B978-0-444-53159-9.00010-3>

722 Du Laing, G., Rinklebe, J., Vandecasteele, B., Meers, E., Tack, F.M.G., 2009. Trace metal behaviour in
723 estuarine and riverine floodplain soils and sediments: A review. *Sci. Total Environ.* 407, 3972–
724 3985. <https://doi.org/10.1016/J.SCITOTENV.2008.07.025>

725 Du Laing, G., Vanthuyne, D.R.J., Vandecasteele, B., Tack, F.M.G., Verloo, M.G., 2007. Influence of

hydrological regime on pore water metal concentrations in a contaminated sediment-derived soil. *Environ. Pollut.* 147, 615–625. <https://doi.org/10.1016/J.ENVPOL.2006.10.004>

Emerson, Kodak U, Scholastica Bejor, E., Ekeng, E.E., Ogarekpe, Nkpa M, Emerson, K U, Bejor, E.S., Ogarekpe, N M, Onuruka, A.U., 2017. TRANSPORT AND FATE OF SELECTED HEAVY METALS IN CIRCUMNEUTRAL RIVER ENVIRONMENT: A CASE STUDY OF THE RIVER NENT CUMBRIA, ENGLAND. *Int. J. Res.* 5, 159–169. <https://doi.org/10.5281/zenodo.818628>

Förstner, U., 2004. Traceability of sediment analysis. *TrAC Trends Anal. Chem.* 23, 217–236. [https://doi.org/10.1016/S0165-9936\(04\)00312-7](https://doi.org/10.1016/S0165-9936(04)00312-7)

Frohne, T., Diaz-Bone, R.A., Du Laing, G., Rinklebe, J., 2015. Impact of systematic change of redox potential on the leaching of Ba, Cr, Sr, and V from a riverine soil into water. *J. Soils Sediments* 15, 623–633. <https://doi.org/10.1007/s11368-014-1036-8>

Frohne, T., Rinklebe, J., Diaz-Bone, R.A., Du Laing, G., 2011. Controlled variation of redox conditions in a floodplain soil: Impact on metal mobilization and biomethylation of arsenic and antimony. *Geoderma* 160, 414–424. <https://doi.org/10.1016/J.GEODERMA.2010.10.012>

Furman, O., Strawn, D.G., McGeehan, S., 2007. Sample Drying Effects on Lead Bioaccessibility in Reduced Soil. *J. Environ. Qual.* 36, 899–903. <https://doi.org/10.2134/jeq2006.0340>

González-Alcaraz, M.N., van Gestel, C.A.M., 2015. Climate change effects on enchytraeid performance in metal-polluted soils explained from changes in metal bioavailability and bioaccumulation. *Environ. Res.* 142, 177–184. <https://doi.org/10.1016/j.envres.2015.06.027>

Grybos, M., Davranche, M., Gruau, G., Petitjean, P., Pédrot, M., 2009. Increasing pH drives organic matter solubilization from wetland soils under reducing conditions. *Geoderma* 154, 13–19. <https://doi.org/10.1016/j.geoderma.2009.09.001>

He, J., Yang, Y., Christakos, G., Liu, Y., Yang, X., 2019. Assessment of soil heavy metal pollution using stochastic site indicators. *Geoderma* 337, 359–367. <https://doi.org/10.1016/J.GEODERMA.2018.09.038>

Hooda, P.S., 2010. Trace Elements in Soils, Trace Elements in Soils. John Wiley and Sons. <https://doi.org/10.1002/9781444319477>

Hurley, R.R., Rothwell, J.J., Woodward, J.C., 2017. Metal contamination of bed sediments in the Irwell and Upper Mersey catchments, northwest England: exploring the legacy of industry and urban growth. *J. Soils Sediments* 17, 2648–2665. <https://doi.org/10.1007/s11368-017-1668-6>

756 Icopini, G.A., Long, D.T., 2002. Speciation of aqueous chromium by use of solid-phase extractions in
757 the field. *Environ. Sci. Technol.* 36, 2994–2999. <https://doi.org/10.1021/es015655u>

758 Indraratne, S.P., Kumaragamage, D., 2017. Flooding-induced mobilization of potentially toxic trace
759 elements from uncontaminated, calcareous agricultural soils. *Can. J. Soil. Sci.* 98, 103–113.
760 <https://doi.org/10.1139/cjss-2017-0077>

761 Izquierdo, M., Tye, A.M., Chenery, S.R., 2017. Using isotope dilution assays to understand speciation
762 changes in Cd, Zn, Pb and Fe in a soil model system under simulated flooding conditions.
763 *Geoderma* 295, 41–52. <https://doi.org/10.1016/J.GEODERMA.2017.02.006>

764 Kashem, M.A., Singh, B.R., 2001. Metal availability in contaminated soils: I. Effects of flooding and
765 organic matter on changes in Eh, pH and solubility of Cd, Ni and Zn. *Nutr. Cycl. Agroecosystems*
766 61, 247–255. <https://doi.org/10.1023/A:1013762204510>

767 Kelly, T.J., Hamilton, E., Watts, M.J., Ponting, J., Sizmur, T., 2020. The effect of flooding and drainage
768 duration on the release of trace elements from floodplain soils. *Environ. Toxicol. Chem.*
769 etc.4830. <https://doi.org/10.1002/etc.4830>

770 Kotuby-Amacher, J., Gambrell, R.P., 1989. Factors affecting trace-metal mobility in subsurface soils.
771 *LSU Hist. Diss. Theses* 4787.

772 Koupai, J.A., Fatahizadeh, M., Mosaddeghi, M.R., 2020. Effect of pore water pH on mechanical
773 properties of clay soil. *Bull. Eng. Geol. Environ.* 79, 1461–1469.
774 <https://doi.org/10.1007/s10064-019-01611-1>

775 Lair, G.J., Zehetner, F., Fiebig, M., Gerzabek, M.H., van Gestel, C.A.M., Hein, T., Hohensinner, S., Hsu,
776 P., Jones, K.C., Jordan, G., Koelmans, A.A., Poot, A., Slijkerman, D.M.E., Totsche, K.U., Bondar-
777 Kunze, E., Barth, J.A.C., 2009. How do long-term development and periodical changes of river-
778 floodplain systems affect the fate of contaminants? Results from European rivers. *Environ.*
779 *Pollut.* 157, 3336–3346. <https://doi.org/10.1016/j.envpol.2009.06.004>

780 Lee, D.Y., Huang, J.C., Juang, K.W., Tsui, L., 2005. Assessment of phytotoxicity of chromium in
781 flooded soils using embedded selective ion exchange resin method. *Plant Soil* 277, 97–105.
782 <https://doi.org/10.1007/s11104-005-5997-7>

783 Lynch, S., Batty, L., Byrne, P., 2014. Environmental Risk of Metal Mining Contaminated River Bank
784 Sediment at Redox-Transitional Zones. *Minerals* 4, 52–73. <https://doi.org/10.3390/min4010052>

785 Maranguit, D., Guillaume, T., Kuzyakov, Y., 2017. Effects of flooding on phosphorus and iron

786 mobilization in highly weathered soils under different land-use types: Short-term effects and
787 mechanisms. *Catena* 158, 161–170. <https://doi.org/10.1016/j.catena.2017.06.023>

788 Matern, K., Mansfeldt, T., 2016. Chromate adsorption from chromite ore processing residue eluates
789 by three Indian soils. *Environ. Chem.* 13, 674. <https://doi.org/10.1071/EN15147>

790 Mohamed, A.-M.O., Paleologos, E.K., 2018. The Soil System, in: *Fundamentals of Geoenvironmental*
791 *Engineering*. Elsevier, pp. 89–127. <https://doi.org/10.1016/b978-0-12-804830-6.00004-1>

792 Moser, K., Ahn, C., Noe, G., 2007. Characterization of microtopography and its influence on
793 vegetation patterns in created wetlands. *Wetlands* 27, 1081–1097.

794 Mulligan, C.N., Yong, R.N., Gibbs, B.F., 2001. Remediation technologies for metal-contaminated soils
795 and groundwater: An evaluation. *Eng. Geol.* 60, 193–207. [https://doi.org/10.1016/S0013-](https://doi.org/10.1016/S0013-7952(00)00101-0)
796 [7952\(00\)00101-0](https://doi.org/10.1016/S0013-7952(00)00101-0)

797 Newsome, L., Solano Arguedas, A., Coker, V.S., Boothman, C., Lloyd, J.R., 2020. Manganese and
798 cobalt redox cycling in laterites; Biogeochemical and bioprocessing implications. *Chem. Geol.*
799 531, 119330. <https://doi.org/10.1016/j.chemgeo.2019.119330>

800 O’Connell, E., Ewen, J., O’Donnell, G., Quinn, P., 2007. Is there a link between agricultural land-use
801 management and flooding? *Hydrol. Earth Syst. Sci.* 11, 96–107. [https://doi.org/10.5194/hess-](https://doi.org/10.5194/hess-11-96-2007)
802 [11-96-2007](https://doi.org/10.5194/hess-11-96-2007)

803 Ortiz Colon, A.I., 2016. Assessment of Concentrations of Heavy Metals and Phthalates in Two Urban
804 Rivers of the Northeast of Puerto Rico. *J. Environ. Anal. Toxicol.* 06.
805 <https://doi.org/10.4172/2161-0525.1000353>

806 Palansooriya, K.N., Shaheen, S.M., Chen, S.S., Tsang, D.C.W., Hashimoto, Y., Hou, D., Bolan, N.S.,
807 Rinklebe, J., Ok, Y.S., 2020. Soil amendments for immobilization of potentially toxic elements in
808 contaminated soils: A critical review. *Environ. Int.* 134, 105046.
809 <https://doi.org/10.1016/j.envint.2019.105046>

810 Ponting, J., Kelly, T.J., Verhoef, A., Watts, M.J., Sizmur, T., 2021. The impact of increased flooding
811 occurrence on the mobility of potentially toxic elements in floodplain soil – A review. *Sci. Total*
812 *Environ.* 754, 142040. <https://doi.org/10.1016/j.scitotenv.2020.142040>

813 Prabakaran, K., Nagarajan, R., Eswaramoorthi, S., Anandkumar, A., Franco, F.M., 2019.
814 Environmental significance and geochemical speciation of trace elements in Lower Baram River
815 sediments. *Chemosphere* 219, 933–953. <https://doi.org/10.1016/j.chemosphere.2018.11.158>

816 Rawlins, B.G., McGrath, S.P., Scheib, A.J., Breward, N., Cave, M., Lister, T.R., Ingham, M., Gowing, C.,
817 Carter, S., 2012. The advanced soil geochemical atlas of England and Wales. Nottingham, UK,
818 British Geological Survey.

819 Rennert, T., Rabus, W., Rinklebe, J., 2017. Modelling the concentrations of dissolved contaminants
820 (Cd, Cu, Ni, Pb, Zn) in floodplain soils. *Environ. Geochem. Health* 39, 331–344.
821 <https://doi.org/10.1007/s10653-016-9859-4>

822 Resongles, E., Casiot, C., Freydier, R., Le Gall, M., Elbaz-Poulichet, F., 2015. Variation of dissolved and
823 particulate metal(loid) (As, Cd, Pb, Sb, Tl, Zn) concentrations under varying discharge during a
824 Mediterranean flood in a former mining watershed, the Gardon River (France). *J. Geochemical*
825 *Explor.* 158, 132–142. <https://doi.org/10.1016/J.GEXPLO.2015.07.010>

826 Rinklebe, J., Du Laing, G., 2011. Factors Controlling the Dynamics of Trace Metals in Frequently
827 Flooded Soils, in: *Dynamics and Bioavailability of Heavy Metals in the Rootzone*. CRC Press,
828 Taylor & Francis Group, New York, pp. 245–270. <https://doi.org/10.1201/b10796-10>

829 Rinklebe, J., During, A., Overesch, M., Du Laing, G., Wennrich, R., Stärk, H.J.H.J., Mothes, S., 2010.
830 Dynamics of mercury fluxes and their controlling factors in large Hg-polluted floodplain areas.
831 *Environ. Pollut.* 158, 308–318. <https://doi.org/10.1016/j.envpol.2009.07.001>

832 Rinklebe, J., Knox, A.S., Paller, M., Knox, A.S., Paller, M., 2016. Potential Mobility, Bioavailability, and
833 Plant Uptake of Toxic Elements in Temporary Flooded Soils, in: Rinklebe, J. (Ed.), *Trace*
834 *Elements in Waterlogged Soils and Sediments*. CRC Press, Taylor & Francis Group, New York,
835 pp. 303–328. <https://doi.org/10.1201/9781315372952-23>

836 Rinklebe, J., Shaheen, S.M., 2017. Redox chemistry of nickel in soils and sediments: A review.
837 *Chemosphere* 179, 265–278. <https://doi.org/10.1016/J.CHEMOSPHERE.2017.02.153>

838 Rowland, P., Neal, C., Sleep, D., Vincent, C., Scholefield, P., 2011. Chemical Quality Status of Rivers
839 for the Water Framework Directive: A Case Study of Toxic Metals in North West England. *Water*
840 3, 649–666. <https://doi.org/10.3390/w3020650>

841 Santoro, A., Held, A., Linsinger, T.P.J., Perez, A., Ricci, M., 2017. Comparison of total and aqua regia
842 extractability of heavy metals in sewage sludge: The case study of a certified reference
843 material. *Trends Anal. Chem.* 89, 34. <https://doi.org/10.1016/J.TRAC.2017.01.010>

844 Schober, B., Hauer, C., Habersack, H., 2020. Floodplain losses and increasing flood risk in the context
845 of recent historic land use changes and settlement developments: Austrian case studies. *J.*

846 Flood Risk Manag. e12610. <https://doi.org/10.1111/jfr3.12610>

847 Schumann, G.J.P., Muhlhausen, J., Andreadis, K.M., 2019. Rapid Mapping of Small-Scale River-
848 Floodplain Environments Using UAV SfM Supports Classical Theory.
849 <https://doi.org/10.3390/rs11080982>

850 Shaheen, S.M., Rinklebe, J., 2014. Geochemical fractions of chromium, copper, and zinc and their
851 vertical distribution in floodplain soil profiles along the Central Elbe River, Germany. *Geoderma*
852 228–229, 142–159. <https://doi.org/10.1016/J.GEODERMA.2013.10.012>

853 Shaheen, S.M., Rinklebe, J., Frohne, T., White, J.R., DeLaune, R.D., 2016. Redox effects on release
854 kinetics of arsenic, cadmium, cobalt, and vanadium in Wax Lake Deltaic freshwater marsh soils.
855 *Chemosphere* 150, 740–748. <https://doi.org/10.1016/J.CHEMOSPHERE.2015.12.043>

856 Shaheen, S.M., Rinklebe, J., Rupp, H., Meissner, R., 2014. Temporal dynamics of pore water
857 concentrations of Cd, Co, Cu, Ni, and Zn and their controlling factors in a contaminated
858 floodplain soil assessed by undisturbed groundwater lysimeters. *Environ. Pollut.* 191, 223–231.
859 <https://doi.org/10.1016/J.ENVPOL.2014.04.035>

860 Sherene, T., 2010. Mobility and Transport of Heavy Metals in Polluted Soil Environment. *Biol. Forum*
861 *Int. J.* 2, 112–121.

862 Simms, P.H., Yanful, E.K., St-Arnaud, L., Aubeâ, B., 2000. A laboratory evaluation of metal release and
863 transport in flooded pre-oxidized mine tailings. *Appl. Geochemistry* 15, 1245–1263.

864 Sizmur, T., Campbell, L., Dracott, K., Jones, M., O’Driscoll, N.J., Gerwing, T., 2019. Relationships
865 between Potentially Toxic Elements in intertidal sediments and their bioaccumulation by
866 benthic invertebrates. *PLoS One* 14, e0216767. <https://doi.org/10.1371/journal.pone.0216767>

867 Sizmur, T., Palumbo-Roe, B., Hodson, M.E., 2011. Impact of earthworms on trace element solubility
868 in contaminated mine soils amended with green waste compost. *Environ. Pollut.* 159, 1852–
869 1860. <https://doi.org/10.1016/j.envpol.2011.03.024>

870 Small, C.C., Woosaree, J., Naeth, M.A., 2015. Assessing reclamation ready tailings materials using
871 outdoor terrestrial mesocosms, in: *Tailings and Mine Waste Conference*. Vancouver British
872 Columbia.

873 Sparovek, G., De Jong van Lier, Q., Marcinkonis, S., Rogasik, J., Schnug, E., 2002. A simple model to
874 predict river floods - A contribution to quantify the significance of soil infiltration rates. *FAL -*
875 *Agric. Res.* 52, 187–194.

876 Stafford, A., Jeyakumar, P., Hedley, M., Anderson, C., 2018. Influence of Soil Moisture Status on Soil
877 Cadmium Phytoavailability and Accumulation in Plantain (*Plantago lanceolata*). *Soil Syst.* 2, 9.
878 <https://doi.org/10.3390/soils2010009>

879 Stietiya, M.H., 2010. Sorption mechanisms of zinc in different clay minerals and soil systems as
880 influenced by various natural ligands. LSU Dr. Diss. Louisiana State University.

881 Strawn, D.G., 2018. Review of interactions between phosphorus and arsenic in soils from four case
882 studies. *Geochem. Trans.* <https://doi.org/10.1186/s12932-018-0055-6>

883 Stuart, M., Lapworth, D., 2011. A review of processes important in the floodplain setting. *Br. Geol.*
884 *Surv.* 32 (OR/11/030).

885 Szabó, Z., Buró, B., Szabó, J., Tóth, C.A., Baranyai, E., Herman, P., Prokisch, J., Tomor, T., Szabó, S.,
886 2020. Geomorphology as a Driver of Heavy Metal Accumulation Patterns in a Floodplain. *Water*
887 12, 563. <https://doi.org/10.3390/w12020563>

888 Tack, F.M.G., 2010. Trace elements: General soil chemistry, principles and processes, in: *Trace*
889 *Elements in Soils*. John Wiley and Sons, pp. 9–37. <https://doi.org/10.1002/9781444319477.ch2>

890 The Wildlife Trusts Hampshire & Isle of Wight, 2003. *Biodiversity Strategy: The Loddon Catchment*.
891 Wokingham.

892 Tóth, G., Hermann, T., Da Silva, M.R., Montanarella, L., 2016. Heavy metals in agricultural soils of the
893 European Union with implications for food safety. *Environ. Int.* 88, 299–309.
894 <https://doi.org/10.1016/J.ENVINT.2015.12.017>

895 Trebien, D.O.P., Bortolon, L., Tedesco, M.J., Bissani, C.A., Camargo, F.A.O., 2011. Environmental
896 Factors Affecting Chromium-Manganese Oxidation-Reduction Reactions in Soil. *Pedosphere* 21,
897 84–89. [https://doi.org/10.1016/S1002-0160\(10\)60082-3](https://doi.org/10.1016/S1002-0160(10)60082-3)

898 Van Groeningen, N., Glück, B., Christl, I., Kretzschmar, R., 2020. Surface precipitation of Mn²⁺ on clay
899 minerals enhances Cd²⁺ sorption under anoxic conditions. *Environ. Sci. Process. Impacts* 22,
900 1654–1665. <https://doi.org/10.1039/d0em00155d>

901 Weber, F.-A., Voegelin, A., Kretzschmar, R., 2009. Multi-metal contaminant dynamics in temporarily
902 flooded soil under sulfate limitation. *Geochim. Cosmochim. Acta* 73, 5513–5527.
903 <https://doi.org/10.1016/J.GCA.2009.06.011>

904 Williams, P.N., Zhang, H., Davison, W., Meharg, A.A., Hossain, M., Norton, G.J., Brammer, H., Rafiqul,
905 M., || I., 2011. Organic Matter-Solid Phase Interactions Are Critical for Predicting Arsenic

906 Release and Plant Uptake in Bangladesh Paddy Soils. *Environ. Sci. Technol* 45, 6080–6087.
 907 <https://doi.org/10.1021/es2003765>

908 Wood, C.W., Adams, J.F., Wood, B.H., 2004. Macronutrients, in: Hillel, D., Hatfield, J.L., Powlson,
 909 D.S., Rosenzweig, C., Scow, K.M., Singer, M.J., Sparks, D.. (Eds.), *Encyclopedia of Soils in the*
 910 *Environment*. Elsevier Ltd, pp. 387–393. <https://doi.org/10.1016/B0-12-348530-4/00278-2>

911 Wuana, R.A., Okieimen, F.E., Montuelle, B., Steinman, A.D., 2011. Heavy Metals in Contaminated
 912 Soils: A Review of Sources, Chemistry, Risks and Best Available Strategies for Remediation. *Int.*
 913 *Sch. Res. Netw. ISRN Ecol.* 2011, 20. <https://doi.org/10.5402/2011/402647>

914 Zhang, J., Chen, L., Yin, H., Jin, S., Liu, F., Chen, H., 2017. Mechanism study of humic acid functional
 915 groups for Cr(VI) retention: Two-dimensional FTIR and ¹³C CP/MAS NMR correlation
 916 spectroscopic analysis. *Environ. Pollut.* 225, 86–92.
 917 <https://doi.org/10.1016/J.ENVPOL.2017.03.047>

918 Zia-ur-Rehman, M., Sabir, M., Rizwan, M., Saifullah, Ahmed, H.R., Nadeem, M., 2015. Remediating
 919 Cadmium-Contaminated Soils by Growing Grain Crops Using Inorganic Amendments, in: *Soil*
 920 *Remediation and Plants: Prospects and Challenges*. Elsevier Inc., pp. 367–396.
 921 <https://doi.org/10.1016/B978-0-12-799937-1.00013-9>

922